



Estimation of Earth Rotation Parameter UT1 from Lunar Laser Ranging Observations

Liliane Biskupek, Vishwa Vijay Singh, and Jürgen Müller

Abstract

Since 1969 Lunar Laser Ranging (LLR) data have been collected by different observatories and analysed by various analysis groups. LLR is providing the longest time series of any space geodetic technique for studying the Earth-Moon dynamics. In recent years, observations have been carried out with larger telescopes and at infra-red (IR) wavelength, resulting in a better distribution of precise LLR data over the lunar orbit and the observed retro-reflectors on the Moon. The increased number of high-accuracy observations allows for more accurate determination of Earth Orientation Parameters (EOPs) from LLR data compared to previous years. In this study we focus on Δ UT1 results from different constellations and compare our LLR solution to the IERS EOP C04 series.

Keywords

Earth rotation parameters · Earth rotation phase · Lunar laser ranging

1 Introduction

With the landing of Apollo 11 astronauts on the Moon in July 1969 the first LLR retro-reflector was deployed on the lunar surface. Until 1973, four additional retro-reflectors had been installed on the Moon: two reflectors by the astronauts of the Apollo 14 and 15 missions, and two reflectors mounted on the unmanned Soviet Lunokhod rovers. Measurements from the Earth to the retro-reflectors have primarily been carried out from six observatories that were or are capable to range to the Moon: the McDonald Laser Ranging Station, USA (MLRS), the Lure Observatory on Maui/Hawaii, USA (LURE), the Côte d'Azur Observatory, France (OCA), the

Apache Point Observatory Lunar Laser ranging Operation, USA (APOLLO), the Matera Laser Ranging Observatory, Italy (MLRO) and the Geodetic Observatory Wettzell, Germany (WLRS). For more than 52 years now, there are LLR measurements of the round-trip travel time of laser pulses between observatories on the Earth and retro-reflectors on the Moon. The measurement of round trip travel times with short laser pulses is challenging. The average number of returning photons is less than one per laser pulse (Chabé et al. 2020; Murphy 2013), mainly because of the beam divergence of the laser pulses due to the atmospheric turbulence and diffraction effects of the retro-reflectors (Murphy et al. 2010). Further signal loss occurs in the paths of the transmitting and detection optics, in the atmosphere and due to the reflectivity of the retro-reflectors (Müller et al. 2019). A series of single measurements over 5 min to 15 min is used to calculate a so-called normal point (NP) (Michelsen 2010) which is the observable in the LLR analysis. Analysing the data, various research questions related to the Earth-Moon system are investigated. Today, LLR is one of the major tools to test General Relativity in the solar system, e.g. testing the equivalence principle, temporal variation of the gravitational constant G , Yukawa term, metric parameters, and geodetic

L. Biskupek (✉) · J. Müller
Institute of Geodesy (IfE), Leibniz University Hannover, Hannover,
Germany
e-mail: biskupek@ife.uni-hannover.de

V.V. Singh
Institute of Geodesy (IfE), Leibniz University Hannover, Hannover,
Germany

Institute for Satellite Geodesy and Inertial Sensing, German Aerospace
Center (DLR), Hannover, Germany

precession (Biskupek et al. 2021; Zhang et al. 2020; Hofmann and Müller 2018; Viswanathan et al. 2018; Williams et al. 2012). Furthermore, LLR can also be used to determine parameters of the Earth-Moon system like its mass, the lunar orbit and libration (Pavlov et al. 2016; Williams et al. 2013), terrestrial and celestial reference frames and the coordinates of observatories and retro-reflectors (Hofmann et al. 2018; Müller et al. 2009). In Germany, beginning in the early 1980s, the software package LUNAR (LUNAr laser ranging Analysis softwaRE) was developed to study the Earth-Moon system and to determine the various related model parameters. In this study we focus on the determination of the Earth rotation parameter ΔUT1 . ΔUT0 is a special case of Universal Time (UT) at a certain location. It can only be measured by LLR as well as Very Long Baseline Interferometry (VLBI).

2 Analysis and Observations

Currently, the analysis of LLR data includes 28,093 NPs for the time span April 1970–April 2021. The temporal distribution of the measured NPs over the last 52 years is given in Fig. 1. One can see in the legend that more than 60% of the NPs were observed by OCA, 40% with green and 21% with IR laser wavelength (measurements with laser wavelength of $\lambda = 693.8\text{ nm}$ and $\lambda = 532\text{ nm}$ are listed in the figure as OCA green). In the last years, only OCA and APOLLO provided regular NPs, some NPs also came from MLRO and WLRS. As of 2015, many NPs were measured with laser pulses at IR wavelength, enabling distance measurements near new and full Moon (Chabé et al. 2020) for OCA and WLRS. This leads to a better coverage of the lunar orbit over the synodic month, i.e. the time span in which the Sun, the Earth, and the Moon return to a similar constellation again. With a better coverage of the lunar orbit, it is possible to

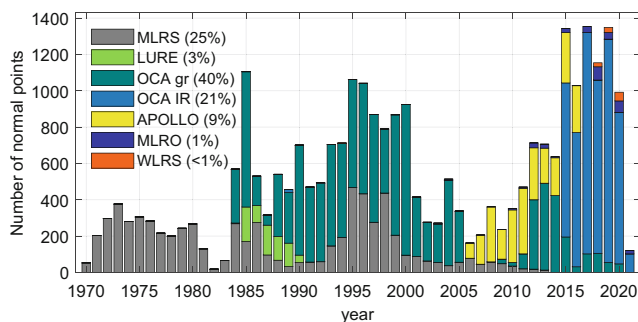


Fig. 1 Distribution of the 28,093 NPs over the time span April 1970–April 2021. The legend gives the percentages of the contribution of the respective observatories. The three observatories McDonald, MLRS1 and MLRS2 are linked in the analysis and listed here as MLRS. OCA measurements with laser wavelength of $\lambda = 693.8\text{ nm}$ and $\lambda = 532\text{ nm}$ are indicated as OCA gr

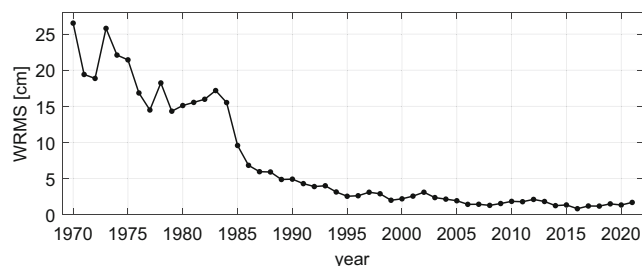


Fig. 2 Annual weighted RMS (WRMS) of the one-way post-fit residuals for 28,093 NPs for the time span April 1970–April 2021

perform a more uniform estimation of various parameters of the Earth-Moon system. Nevertheless the distribution of the NPs has a big impact on the determination of the parameters. Furthermore, non-uniform data distribution is one reason for correlations between solution parameters (Williams et al. 2009). The measured NPs serve as observations in the analysis. They are treated as uncorrelated for the stochastic model of the least-squares adjustment and are weighted according to their accuracies.

In the LLR analysis, the parameters of the LLR model are determined by fitting them to the LLR observations using the least-squares adjustment. The ephemeris of the solar system bodies are integrated simultaneously with the rotation of the Moon. For the rotation of the Earth two series of EOPs are used: until 01.01.1983, the Kalman Earth Orientation Filter (KEOF) series COMB2019 (Ratcliff and Gross 2020) and from 02.01.1983 the IERS EOP C04 series (Bizouard et al. 2019). The difference between the two EOP series is the input data, as only the COMB series includes LLR NPs. Therefore, this series fits the LLR analysis better in the initial phase of the observations. After 01.01.1983, the differences between the two EOP series are small (only a few mas and ms), so that the IERS series is used for timeliness reasons. The coordinates and velocities of the LLR observatories are determined in the International Terrestrial Reference System (ITRS). The weighted RMS of the one-way post-fit residuals of the LLR analysis is better than 1.5 cm for the last years, see Fig. 2.

3 ΔUT1 from LLR

The terrestrial pole coordinates x_p and y_p , describe the change of the rotation axis in relation to the Earth's surface. The rotational motion of the Earth is given by the Earth rotation phase ΔUT1 and the Length-of-Day LOD. All these parameters are summarised as Earth Rotation Parameters (ERPs). Together with the celestial pole offsets δX and δY , as corrections to the conventional precession-nutation model, they define the Earth Orientation Parameter (EOP).

As shown by Dickey et al. (1985), Müller (1991) and Pavlov (2019), it is possible to determine the ERPs from the post-fit residuals of the least-squares adjustment of LLR data. In this way the variation of longitude $\Delta UT0$ can be determined by

$$\Delta UT0 = \Delta UT1 + \frac{(x_p \sin(\lambda) + y_p \cos(\lambda)) \tan(\phi)}{15 \times 1.002737909}, \quad (1)$$

as combination of $\Delta UT1$ and the terrestrial pole coordinates x_p, y_p , with the observatories longitude λ and latitude ϕ (Chapront-Touzé et al. 2000). The variation of latitude VOL is given by

$$VOL = x_p \cos \lambda - y_p \sin \lambda. \quad (2)$$

The disadvantage of this approach is that the correlations between the ERPs and the other parameters of the Earth-Moon system can not be investigated. Biskupek (2015) changed the analysis strategy. In the rotation matrix between the Earth-fixed ITRS and the space-fixed Geocentric Celestial Reference System (GCRS) the ERPs are used in the LLR analysis, thus they can be determined in the least-squares adjustment along with other parameters of the Earth-Moon system. The correlations with these parameters are also obtained and can be investigated directly. Biskupek (2015) gave the equations for the partial derivatives of ERPs and discussed the results of the different possible methods to obtain ERPs from LLR, such as selecting certain time spans of data or specific nights for which a minimum number of NPs is available. The main result of this research was that the determination for specific nights with a minimum of 5 NPs is a better method than the ERP determination for longer time spans. From the analysis of 20,047 NPs (1970–2013), the uncertainty in $\Delta UT1$ was about 400 μ s. Hofmann et al. (2018) discussed the results of estimating the Earth rotation phase for a time span with 23,261 NPs (1970–2016). They achieved an uncertainty of 89 μ s when estimating $\Delta UT1$ from all observatories and of 44 μ s when estimating $\Delta UT1$ from only OCA and APOLLO. The IR measurements from OCA with better coverage of the lunar orbit and more NPs that are available per night lead to an improved situation for the LLR observables. This enables a better and more stable estimation of ERPs from LLR, which achieve lower uncertainties compared to previous results. A further study concerning ERP determination from LLR data with more details is published by Singh et al. (2022).

For ERP determination in the LLR analysis, the whole data set of NPs is pre-analysed, where different configurations can be taken into account. Thus, it is possible to estimate ERPs from the data of all observatories or only for a single observatory. It is also possible to vary the number of NPs per night or to choose specific wavelengths. In the

current study we focused on the determination of the Earth rotation phase $\Delta UT1$. Several studies with different characteristics were performed, like different numbers of NPs per night from different observatories and different combination of the wavelength of the measured NPs. Two studies with the best results are with data from OCA and are discussed in the following.

The main characteristics of the two studies were the same. The $\Delta UT1$ values were determined from the LLR data for specific nights. The minimum number of NPs for one night to be considered in the $\Delta UT1$ determination was set to 10, i.e. nights with fewer NPs were not considered in the fit. Simultaneously, the coordinates of the observatories were determined for one epoch, namely J2000 (01.01.2000, 0:00 UTC), of the whole LLR data set. Theoretically, it is also possible to determine velocities of the observatories from the whole LLR data set. Since there are correlations between $\Delta UT1$, coordinates and velocities on the one hand, as well as large deviations of station coordinates to the ITRF2014 on the other hand, the velocities were fixed to their ITRF2014 values. However, as the APOLLO observatory is not included in the ITRF2014 solution, we used the velocity of the White Sands GNSS observatory instead. The a-priori EOP values were used from COMB2019/IERS C04 series and fixed for those nights that were not considered in the fit. For a complete list of parameters determined together with the $\Delta UT1$ values (e.g. station coordinates and range biases), except the station velocities, see Singh et al. (2021). The difference in the two study cases was the wavelength of the used laser and the resulting different number of nights for the $\Delta UT1$ determination. In study 1 there were 714 nights for the time span April 1984–March 2021 in which NPs were measured with green or IR laser wavelength. For study 2 there were 259 nights for the time span March 2015–March 2021 in which NPs were measured with IR laser wavelength only.

Figure 3 shows the results for the two studies where the deviations from the IERS C04 series and their uncertainties are given. A previous study has shown that the uncertainties of the estimated parameters from our LLR analysis were too small (Hofmann et al. 2018), as some small random and systematic errors remained in the LLR analysis. Systematic errors include the uneven distribution of NPs during the synodic month, and the constellation of Earth and Moon when observing an LLR NP, because of the inaccuracy of atmospheric delay models for low altitude observations. A further error source is the imperfection of lunar ephemeris, e.g. because of simplified modelling of the asteroids. These errors are different for each observation. Random errors result from the general measurement accuracy of LLR, are different for each night, and depend on the observatory measuring the NPs. Furthermore, the $\Delta UT1$ determination is constrained by the a priori EOP series for nights when

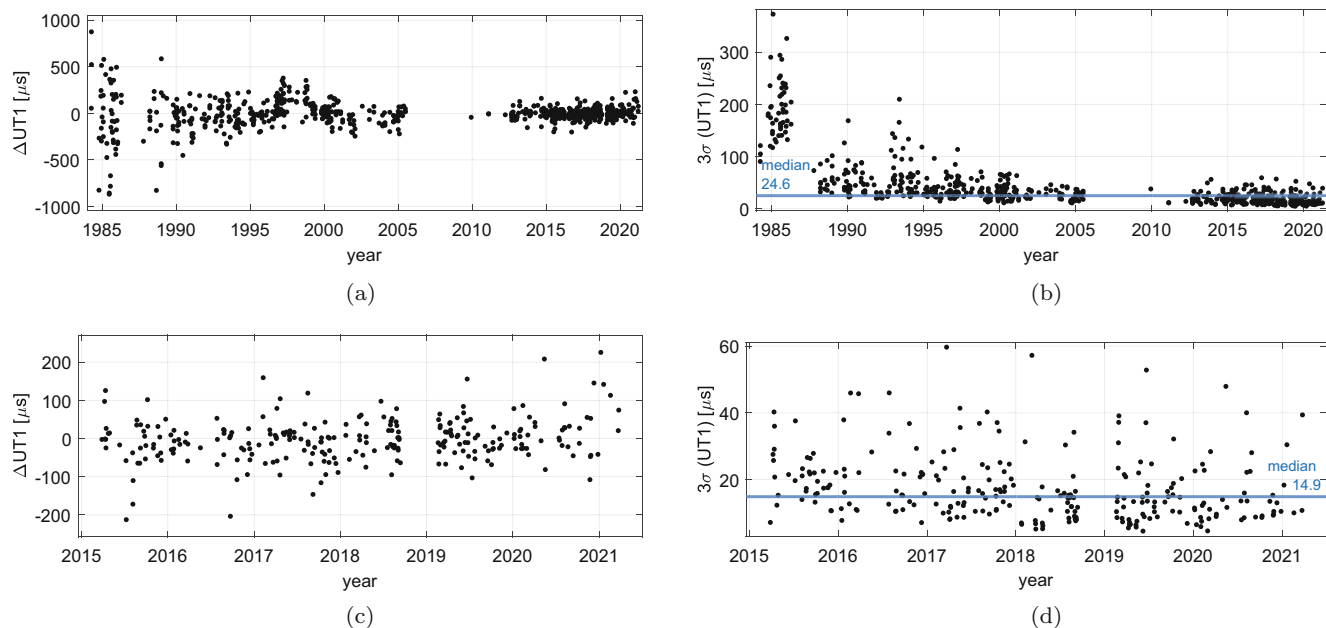


Fig. 3 Results of studies 1 and 2 on the determination of ΔUT1 from LLR data in different configurations. (a) ΔUT1 deviations from the IERS C04 series as determined in study 1 from green and IR NPs. (b) Uncertainty of the ΔUT1 values of study 1 for the individual nights

and the median of all nights. (c) ΔUT1 deviations from the IERS C04 series as determined in study 2 from IR NPs only. (d) Uncertainty of the ΔUT1 values of study 2 for the individual nights and the median of all nights

no values are estimated. Additionally, according to Eq. (1) the pole coordinates also affect ΔUT1 . In our case we fixed the pole coordinates to the IERS C04 series and assumed them to be error-free, which is not the case. The following uncertainties are given as 3 times the formal errors from the least-squares adjustment.

Figure 3a gives the fitted ΔUT1 deviations to the IERS C04 series as determined in study 1, where NPs measured with green or IR laser wavelength were used. The values vary between $\pm 200 \mu\text{s}$ with a mean of $4.3 \mu\text{s}$ and some higher values before the year 2000 due to the poorer measurement accuracy of this period. The RMS is $149.2 \mu\text{s}$. The uncertainties of the ΔUT1 deviations are in the range of $4.5 \mu\text{s}$ to $373.1 \mu\text{s}$ with a median of $24.6 \mu\text{s}$, shown in Fig. 3b. For study 2 using only IR data the fitted ΔUT1 deviations to the IERS C04 series are given in Fig. 3c. The values vary between $\pm 100 \mu\text{s}$ with a mean of $2.7 \mu\text{s}$ and some higher values. The RMS is $56.4 \mu\text{s}$. Figure 3d gives the corresponding uncertainties, which range between $4.5 \mu\text{s}$ to $60.0 \mu\text{s}$ with a median of $14.89 \mu\text{s}$. In previous studies (Hofmann et al. 2018), a higher uncertainty of $32 \mu\text{s}$ was achieved, although in these studies the minimum number of NPs per night was 14 and thus higher than now. Since the time span of used NPs was only until 2016, the very accurate and well distributed OCA NPs measured in IR were not part of that analysis. The advantage of the IR OCA data seems obvious here. They improve the overall uncertainty of the least-squares adjustment and allow

fitting ΔUT1 values with lower uncertainty from less NPs per night.

The influence of the number and accuracy of the NPs on the determination of ΔUT1 is analysed in more detail in Fig. 4 where scatter plots show the relationship between the number or accuracy of the NPs and the uncertainty of ΔUT1 . Correlation coefficients were determined from each combination of data sets that are given in the plots. The accuracies of the input NPs were averaged for each night considered and plotted on the horizontal axis of Fig. 4b and d. In study 1 with NPs measured with green or IR laser wavelength, the number of NPs does not have a very large effect on the uncertainty of ΔUT1 (see Fig. 4a), the correlation coefficient is only -0.27 . The accuracy of NPs is more important in this study (see Fig. 4b), as reflected by a correlation coefficient of 0.91 with the uncertainty of ΔUT1 . In study 2, using only IR NPs with a more homogeneous accuracy between each NP, the correlation coefficient between the accuracy of NPs and the uncertainty of ΔUT1 with 0.41 is lower than in study 1 (see Fig. 4d). Here, the number of NPs has a larger effect compared with study 1 (see Fig. 4c) and the correlation coefficient is -0.43 . This means that for the determination of ΔUT1 a high accuracy of the NPs is beneficial for data sets with inhomogeneous input data accuracy, but also a high number of NPs per night is important in the analysis. Both criteria of the input data play a role in the determination of ΔUT1 .

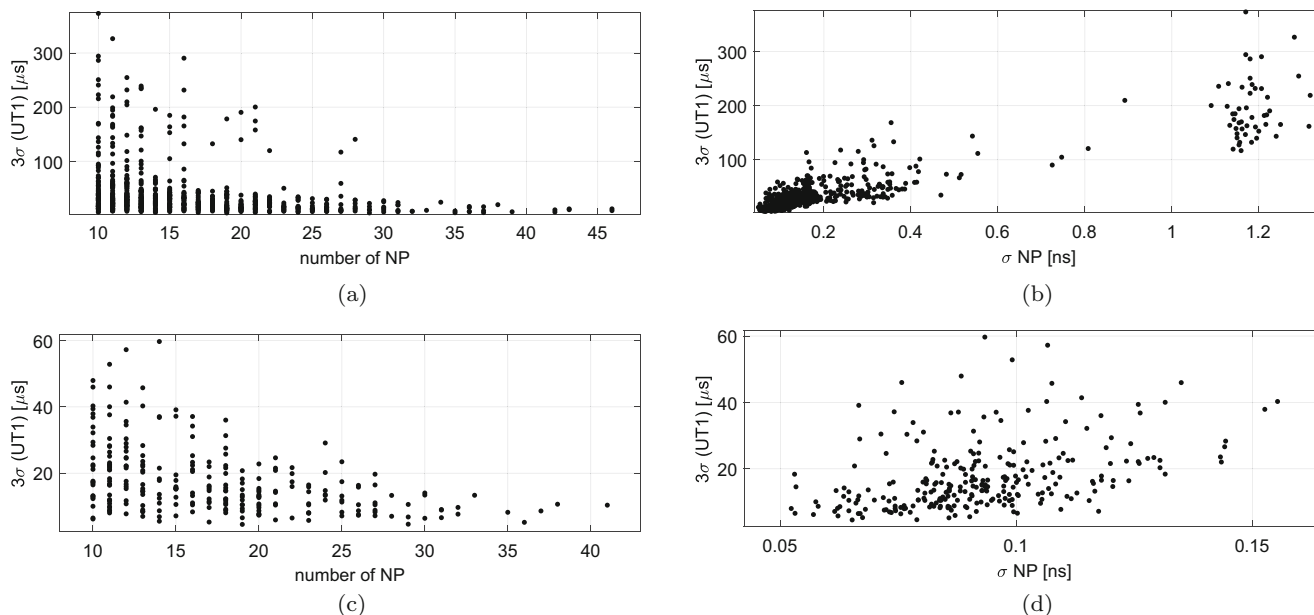


Fig. 4 Different scatter plot for studies 1 and 2 between the LLR NPs and the determined uncertainty of $\Delta UT1$. **(a)** Study 1 (green and IR NPs): Scatter plot of the number of NPs and the estimated uncertainty of $\Delta UT1$. The correlation coefficient is -0.27 . **(b)** Study 1 (green and IR NPs): Scatter plot of the measured accuracy of NPs and the estimated

uncertainty of $\Delta UT1$. The correlation coefficient is 0.91 . **(c)** Study 2 (IR NPs only): Scatter plot of the number of NPs and the estimated uncertainty of $\Delta UT1$. The correlation coefficient is -0.43 . **(d)** Study 2 (IR NPs only): Scatter plot of the measured accuracy of NPs and the estimated uncertainty of $\Delta UT1$. The correlation coefficient is 0.41

In both studies, no significant correlations of $\Delta UT1$ values and other parameters of the Earth-Moon system were found in the least-squares adjustment. Comparable results for $\Delta UT1$ with an uncertainty of $15 \mu s$ are obtained from VLBI data (Gambis and Luzum 2011).

4 Conclusions

As described above ERPs can be determined from LLR data analysis. The best LLR result is obtained from the high-accurate IR OCA data with 10 NPs per night with a median uncertainty of $14.89 \mu s$. The high-accurate IR data from OCA are very beneficial for the $\Delta UT1$ determination, because of their distribution over the reflectors and synodic month as well as the higher number of NPs for one night. The data reduce the overall uncertainty of the least-squares adjustment and allow fitting $\Delta UT1$ values with lower uncertainty from fewer NPs per night compared to previous studies.

Deviations from the IERS C04 series are in the range of $\pm 100 \mu s$ at best, with a mean of $2.7 \mu s$ and an RMS of $56.4 \mu s$. The mean uncertainty is $14.89 \mu s$. These LLR results are in a range of uncertainty which is comparable to daily $\Delta UT1$ values determined from VLBI with $15 \mu s$ (Gambis and Luzum 2011). Nevertheless the LLR uncertainties seem to be too optimistic. Therefore as next step, $\Delta UT1$ and also values for pole coordinates from all LLR stations will be determined together and analysed to find the best strategy

for ERP determination from LLR data. It will also be further investigated, which parameters of the Earth-Moon system should be determined together with the ERPs. This will lead to a more realistic estimation of their uncertainties.

With more IR data from the observatories OCA and WLRS, it is expected that the parameters of the least-squares adjustment can be further decorrelated and then station velocities might be determined along with ERPs and station coordinates. Additionally an optimised strategy regarding the number and accuracy of NPs per night is investigated (Singh et al. 2022).

Acknowledgements We acknowledge with gratitude, that more than 52 years of processed LLR data have been obtained under the efforts of the personnel at McDonald Laser Ranging Station, USA, Côte d’Azur Observatory, France, Lure Observatory on Maui/Hawaii, USA, Apache Point Observatory Lunar Laser ranging Operation, USA, Matera Laser Ranging Observatory, Italy and Geodetic Observatory Wettzell, Germany. We also acknowledge with thanks the funding by the Deutsche Forschungsgemeinschaft (DFG, German Research Foundation) under Germany’s Excellence Strategy (EXC-2123 QuantumFrontiers—Project-ID 390837967).

Funding This research was funded by the Deutsche Forschungsgemeinschaft (DFG, German Research Foundation) under Germany’s Excellence Strategy (EXC-2123 QuantumFrontiers—Project-ID 390837967), and Deutsches Zentrum für Luft- und Raumfahrt (DLR).

Conflict of Interest The authors declare that they have no conflict of interest.

Data Availability LLR data is collected, archived, and distributed under the auspices of the International Laser Ranging Service (ILRS)

(Pearlman et al. 2019). All LLR NPs used for these studies are available from the Crustal Dynamics Data Information System (CDDIS) at NASA's Archive for Space Geodesy Data, USA, (Noll 2010) at the website.¹ The KEOF COMB2019 EOP time series is available at the website² and the IERS C04 EOP time series is available at the website.³

Code Availability All calculations were done by unpublished custom code.

Authors' Contributions All authors contributed to the development of these studies and provided ideas to its content. Data collection and analysis were performed by VVS and LB. The first draft of the manuscript was written by LB, and all authors commented on previous versions of the manuscript. All authors read and approved the final manuscript.

References

- Biskupek L (2015) Bestimmung der Erdorientierung mit Lunar Laser Ranging. PhD thesis, Leibniz Universität Hannover. <https://doi.org/10.15488/4721>, Deutsche Geodätische Kommission bei der Bayerischen Akademie der Wissenschaften, Reihe C, Nr. 742
- Biskupek L, Müller J, Torre JM (2021) Benefit of new high-precision LLR data for the determination of relativistic parameters. *Universe* 7(2). <https://doi.org/10.3390/universe7020034>
- Bizouard C, Lambert S, Gattano C, Becker O, Richard JY (2019) The IERS EOP 14C04 solution for Earth orientation parameters consistent with ITRF 2014. *J Geodesy* 93(5):621–633. <https://doi.org/10.1007/s00190-018-1186-3>
- Chabé J, Courde C, Torre JM, Bouquillon S, Bourgoïn A, Aimar M, Albanése D, Chauvineau B, Maríey H, Martinot-Lagarde G, Maurice N, Phung DH, Samain E, Viot H (2020) Recent progress in Lunar Laser Ranging at Grasse Laser Ranging Station. *Earth Space Sci* 7(3):e2019EA000785. <https://doi.org/10.1029/2019EA000785>
- Chapront-Touzé M, Chapront J, Francou G (2000) Determination of UT0 with LLR observations. In: *Proceedings of the Journées 1999 "Motion of Celestial Bodies, Astrometry and Astronomical Reference Frames"*, pp 217–220
- Dickey JO, Newhall XX, Williams JG (1985) Earth orientation from Lunar Laser Ranging and an error analysis of Polar motion services. *J Geophys Res* 90(B11):9353–9362
- Gambis D, Luzum B (2011) Earth rotation monitoring, UT1 determination and prediction. *Metrologia* 48(4):S165–S170
- Hofmann F, Müller J (2018) Relativistic tests with Lunar Laser Ranging. *Classical Quantum Gravity* 35(3):035015. <https://doi.org/10.1088/1361-6382/aa8f7a>
- Hofmann F, Biskupek L, Müller J (2018) Contributions to reference systems from Lunar Laser Ranging using the IfE analysis model. *J Geodesy* 92(9):975–987. <https://doi.org/10.1007/s00190-018-1109-3>
- Michelsen EL (2010) Normal point generation and first photon bias correction in APOLLO Lunar Laser Ranging. PhD thesis, University of California, San Diego
- Müller J (1991) Analyse von Lasermessungen zum Mond im Rahmen einer post-Newton'schen Theorie. PhD thesis, Technische Universität München, Deutsche Geodätische Kommission bei der Bayerischen Akademie der Wissenschaften, Reihe C, Nr. 383
- Müller J, Biskupek L, Oberst J, Schreiber U (2009) Contribution of Lunar Laser Ranging to realise geodetic reference systems. In: Drewes H (ed) *Geodetic reference frames*. International Association of Geodesy Symposia, vol 134. Springer, Berlin, Heidelberg, pp 55–59. <https://doi.org/10.1007/978-3-642-00860-3>
- Müller J, Murphy TW, Schreiber U, Shelus PJ, Torre JM, Williams JG, Boggs DH, Bouquillon S, Bourgoïn A, Hofmann F (2019) Lunar Laser Ranging: a tool for general relativity, lunar geophysics and Earth science. *J Geodesy* 93(11):2195–2210. <https://doi.org/10.1007/s00190-019-01296-0>
- Murphy TW (2013) Lunar Laser Ranging: the millimeter challenge. *Rep Progress Phys* 76(7):076901
- Murphy TW, Adelberger EG, Battat JBR, Hoyle CD, McMillan RJ, Michelsen EL, Samad RL, Stubbs CW, Swanson HE (2010) Long-term degradation of optical devices on the Moon. *Icarus* 208(1):31–35. <https://doi.org/10.1016/j.icarus.2010.02.015>
- Noll CE (2010) The crustal dynamics data information system: A resource to support scientific analysis using space geodesy. *Adv Space Res* 45(12):1421–1440. <https://doi.org/10.1016/j.asr.2010.01.018>
- Pavlov DA (2019) Role of Lunar Laser Ranging in realization of terrestrial, lunar, and ephemeris reference frames. *J Geodesy* 94(1):5. <https://doi.org/10.1007/s00190-019-01333-y>
- Pavlov DA, Williams JG, Suvorkin VV (2016) Determining parameters of Moon's orbital and rotational motion from LLR observations using GRAIL and IERS-recommended models. *Celest Mech Dyn Astron* 126(1):61–88. <https://doi.org/10.1007/s10569-016-9712-1>
- Pearlman MR, Noll CE, Pavlis EC, Lemoine FG, Combrink L, Degnan JJ, Kirchner G, Schreiber U (2019) The ILRS: approaching 20 years and planning for the future. *J Geodesy* 93(11):2161–2180. <https://doi.org/10.1007/s00190-019-01241-1>
- Ratcliff JT, Gross RS (2020) Combinations of Earth Orientation Measurements: SPACE2019, COMB2019, and POLE2019. Tech. Rep. JPL Publication 20-3, Jet Propulsion Laboratory
- Singh VV, Biskupek L, Müller J, Zhang M (2021) Impact of non-tidal station loading in LLR. *Adv Space Res* 67(12):3925–3941. <https://doi.org/10.1016/j.asr.2021.03.018>
- Singh VV, Biskupek L, Müller J, Zhang M (2022) Earth rotation parameter estimation from LLR. *Adv Space Res*. <https://doi.org/10.1016/j.asr.2022.07.038>
- Viswanathan V, Fienga A, Minazzoli O, Bernus L, Laskar J, Gastineau M (2018) The new lunar ephemeris INPOP17a and its application to fundamental physics. *Mon Not R Astron Soc* 476(2):1877–1888. <https://doi.org/10.1093/mnras/sty096>
- Williams JG, Turyshev SG, Boggs DH (2009) Lunar Laser Ranging tests of the equivalence principle with the Earth and Moon. *Int J Modern Phys D* 18(7):1129–1175. <https://doi.org/10.1142/S021827180901500X>
- Williams JG, Turyshev SG, Boggs DH (2012) Lunar Laser Ranging tests of the equivalence principle. *Classical Quantum Gravity* 29(18):184004
- Williams JG, Boggs DH, Folkner WM (2013) DE430 Lunar orbit, physical librations, and surface coordinates. JPL Interoffice Memorandum IOM 335-JW,DB,WF-20080314-001, Jet Propulsion Laboratory, California Institute of Technology, Pasadena, California
- Zhang M, Müller J, Biskupek L (2020) Test of the equivalence principle for galaxy's dark matter by Lunar Laser Ranging. *Celest Mech Dyn Astron* 132(4):25. <https://doi.org/10.1007/s10569-020-09964-6>

¹https://cddis.nasa.gov/Data_and_Derived_Products/SLR/Lunar_laser_ranging_data.html.

²<https://keof.jpl.nasa.gov/combinations/latest/>.

³<https://www.iers.org/IERS/EN/DataProducts/EarthOrientationData/eop.html>.

Open Access This chapter is licensed under the terms of the Creative Commons Attribution 4.0 International License (<http://creativecommons.org/licenses/by/4.0/>), which permits use, sharing, adaptation, distribution and reproduction in any medium or format, as long as you give appropriate credit to the original author(s) and the source, provide a link to the Creative Commons license and indicate if changes were made.

The images or other third party material in this chapter are included in the chapter's Creative Commons license, unless indicated otherwise in a credit line to the material. If material is not included in the chapter's Creative Commons license and your intended use is not permitted by statutory regulation or exceeds the permitted use, you will need to obtain permission directly from the copyright holder.

